

Bosonic Mode Mixing in the Superconducting State Spectral Function of $\text{Bi}_2\text{Sr}_2\text{CaCu}_2\text{O}_{8+\delta}$

M. R. Norman,¹ H. Ding,^{1,2} J. C. Campuzano,^{1,2} T. Takeuchi,^{1,3} M. Randeria,⁴ T. Yokoya,⁵ T. Takahashi,⁵ T. Mochiku,⁶ and K. Kadowaki^{6,7}

(1) *Materials Sciences Division, Argonne National Laboratory, Argonne, IL 60439*

(2) *Department of Physics, University of Illinois at Chicago, Chicago, IL 60607*

(3) *Department of Crystalline Materials Science, Nagoya University, Nagoya 464-01, Japan*

(4) *Tata Institute of Fundamental Research, Bombay 400005, India*

(5) *Department of Physics, Tohoku University, 980 Sendai, Japan*

(6) *National Research Institute for Metals, Sengen, Tsukuba, Ibaraki 305, Japan*

(7) *Institute of Materials Science, University of Tsukuba, Ibaraki 305, Japan*

Photoemission spectra of $\text{Bi}_2\text{Sr}_2\text{CaCu}_2\text{O}_{8+\delta}$ below T_c show two features near the $(\pi, 0)$ point of the zone: a sharp peak at low energy and a higher binding energy hump. We find that the sharp peak persists at low energy even as one moves towards $(0, 0)$, while the broad hump shows significant dispersion which correlates well with the normal state dispersion. We argue that these features are naturally explained by the mixing of electrons with a bosonic mode which appears only below T_c , and speculate that the latter may be related to the resonance seen in recent neutron data.

PACS numbers: 71.25.Hc, 74.25.Jb, 74.72.Hs, 79.60.Bm

Angle resolved photoemission data on the quasi-two dimensional high temperature superconductors can be interpreted in terms of the one-electron spectral function [1]. This implies that important information about the self-energy Σ , and how it changes from the normal to the superconducting (SC) state, can, in principle, be obtained by analysis of the ARPES lineshape. This obviously has important ramifications in elucidating a proper microscopic theory of high temperature superconductors.

Perhaps the most dramatic effect in this regard is the temperature dependence of the lineshape in Bi2212. A very broad normal state spectrum near the $(\pi, 0)$ point of the zone evolves quite rapidly for $T < T_c$ into a sharp, resolution limited, quasiparticle peak [1] followed at higher binding energies by a dip [2,3] then a hump, the latter corresponding to where the spectrum recovers to its normal state value. Similar effects are observed in tunneling [4].

In this paper we focus on another remarkable difference between the normal state and SC state data which has not been noticed earlier. In Fig. 1, we show spectra for a $T_c = 87\text{K}$ Bi2212 sample along $\Gamma - \bar{M} - Z$, i.e., $(0, 0) - (\pi, 0) - (2\pi, 0)$, (a) in the normal state (105 K) and (b) in the SC state (13 K) from which we note two striking features. First, we see that the low energy peak in the SC state persists over a surprisingly large range in \mathbf{k} -space, even when the normal state spectra have dispersed far from the Fermi energy. For example, the sharp peak is visible at about 40meV even in curve 4 of Fig. 1b, when the corresponding normal state spectrum is peaked 320 meV below E_F . Second, when the hump in the SC state disperses, it essentially follows that of the normal state spectrum.

To highlight these two features, we plot in Fig. 2 the position of the sharp peak and that of the hump in the SC state versus the single (broad) spectral peak position in the normal state. The experimental points in this figure are, by themselves, highly suggestive of the quantum mechanical mixing of two levels in the SC state electronic spectral function. We note the similarity of this plot to the spectrum of an electron interacting with a sharp phonon mode [5] in conventional superconductors. At the same time it is very important to stress that, in marked contrast to the phonon case, the “bosonic mode” seen here appears *only* in the superconducting state, and, as we shall argue below, has a many-body origin.

We will discuss below a phenomenological self-energy for the SC state which incorporates the mixing of electron states with a bosonic mode. The resulting spectral functions are not only able to capture the features of the lineshape for a given \mathbf{k} , but, more importantly, also able to describe the very different dispersions of the sharp peak and the broad hump. Note that, while near k_F the sharp peak is quasiparticle-like in nature, it is mostly bosonic-like once the higher energy hump has begun to disperse. It is likely that this bosonic mode has the same physical origin as that recently observed by neutron scattering in YBCO [6].

The data of Fig. 1 were obtained on high quality slightly overdoped Bi2212 single crystals ($T_c = 87\text{K}$), with measurements carried out at the Synchrotron Radiation Center, Wisconsin, using a high resolution 4m normal incidence monochromator [7]. 22eV photons polarized along $\Gamma - \bar{M}$ (the Cu-O bond direction) were used for both narrow energy scans (resolution FWHM=18 meV) and wide energy scans (FWHM=35 meV). Similar results

were seen on a variety of samples with different doping levels, photon polarizations, and photon energies.

We have already noted above the persistence of the low frequency peak in the SC state from curves 4 through 16 in Fig. 1b, about half of the Brillouin zone. As one moves from either extreme towards \bar{M} (curve 11), (1) the broad hump at high binding energy moves towards E_F and (2) weight is transferred from the hump to the low frequency peak, which is fairly fixed in energy. The same phenomena are also seen along \bar{M} to Y (Fig. 1c).

A potential complication in interpreting these data is the influence of images of the CuO bands (ghosts) caused by the incommensurate superlattice [3,7], since one predicts a Fermi crossing of one of these images near curve 4. The following arguments can be made against such an effect. First, the ghosts are not visible in the normal state in this polarization geometry. They do however become quite visible if the photon polarization is rotated by 45° [3]. Moreover, comparison of superconducting state spectra in these two polarizations indicate that the midpoint of the leading edge in the present polarization (20 meV) is near that of the \bar{M} point, whereas in the 45 degree rotated polarization, the midpoint is 5 meV. The latter value is consistent with the expected gap size on the ghost band for this k value. Second, the intensity at the peak position (35 meV) monotonically rises from Γ with a maximum near \bar{M} , indicating only one spectral feature.

We can also eliminate the two bilayer-split bands as the explanation of the non-trivial lineshape with a peak, dip and hump. First, we recall our earlier results [3] on the intensities of the peak and the hump at \bar{M} as a function of varying photon polarization direction from in to out of plane. The fact that the intensities of both these features scaled together argues against these arising from two different bands. Second, the very different dispersions of the peak and hump noted in this paper also implies the same: if the sharp peak was a second band it must also show up above T_c , but it does not.

We begin our discussion of self-energy effects by recalling earlier work on the SC state lineshape. At low energies, there is a linewidth collapse [8] upon cooling through T_c , leading to resolution limited spectral peaks [1] at $T \ll T_c$. This is most easily understood (at least near k_F) by the freezing out of electron scattering once the SC gap opens up. That is, the electron lines in the Feynman diagram shown in Fig. 3a are gapped. At higher energies (3Δ for the s-wave case) the imaginary part of Σ ($Im\Sigma$), which determines the linewidth, must go back to its normal state value, thus leading to a qualitative explanation [9] of the dip and hump in SC state spectra near k_F . For a gap with nodes, relevant to the cuprates, these arguments have to be modified, since contributions to $Im\Sigma$ exist all the way to zero frequency [10].

More recently, theoretical calculations [11], motivated by the neutron scattering experiments in YBCO [6], have

found a sharp structure in the SC state particle-hole susceptibility (bubble in Fig. 3a). Basically, the dominance of $Q = (\pi, \pi)$ scattering, coupled with the effect of the sign change of the d-wave gap with Q on the BCS coherence factors of the bubble, leads to a sharp resonance at ω_0 between Δ_{max} and $2\Delta_{max}$ ($\Delta_{max} = \Delta_{(\pi,0)}$). In some models there is a true collective mode at frequency ω_0 .

Motivated by the data in Fig. 2 and the above considerations, we incorporate the effect of a bosonic mode on the SC state spectral function, taking proper account of both the real and the imaginary parts of the self energy. We note that the importance of structure in $Re\Sigma$ has not been fully appreciated in the context of high T_c superconductors. A mode at ω_0 leads to a singularity in the SC state $Im\Sigma$ at $\omega_0 + \Delta$. By Kramers-Kronig transformation, this implies a singularity in $Re\Sigma$ at $\omega_0 + \Delta$. This feature in $Re\Sigma$ in turn can lead to an additional pole in the spectral function. A simple way to visualize this is to think of an electron interacting with an Einstein mode at ω_0 [5]. One obtains for this model the well-known dispersion with two branches resulting from the mixing of the electron and the mode, with in general one pole being primarily electron-like in nature and the other being primarily mode-like. In addition, there is no damping for frequencies lower than $\omega_0 + \Delta$.

We model the SC state data using the phenomenological self energy [12]

$$\begin{aligned} Im\Sigma(\omega) &= \Gamma_0 N(|\omega|) + \Gamma_1 N(|\omega| - \omega_0), & |\omega| > \omega_0 + \Delta \\ &= \Gamma_0 N(|\omega|), & \Delta < |\omega| < \omega_0 + \Delta \\ &= 0, & |\omega| < \Delta \end{aligned} \quad (1)$$

where $N(\omega) = \omega/\sqrt{\omega^2 - \Delta^2}$ is the BCS density of states, and

$$\begin{aligned} \pi Re\Sigma(\omega) &= \Gamma_0 N(-\omega) \ln \left[\frac{|\omega - \sqrt{\omega^2 - \Delta^2}|}{\Delta} \right] \\ &+ \Gamma_1 N(\omega_0 - \omega) \ln \left[\frac{|\omega_0 - \omega + \sqrt{(\omega - \omega_0)^2 - \Delta^2}|}{\Delta} \right] \\ &\quad - \{\omega \rightarrow -\omega\} \end{aligned} \quad (2)$$

The spectral function is then [5]

$$\pi A(\omega) = Im \frac{Z\omega + \epsilon}{Z^2(\omega^2 - \Delta^2) - \epsilon^2} \quad (3)$$

with (a complex) $Z(\omega) = 1 - \Sigma(\omega)/\omega$.

Note that at large ω the model has a constant linewidth broadening, so that we are effectively ignoring the ω -dependence of the normal state $Im\Sigma$. We have found that simulations with a large constant $Im\Sigma$, which also take into account background emission, can adequately fit the normal state data (see also [13]). From normal state data, we find that Γ_1 is of order 200 meV along $\Gamma - \bar{M}$. The constant linewidth simplification allows us to directly obtain the dispersion $\epsilon_{\mathbf{k}}$ from tight binding fits to the normal state peak position [3]. Our

final results are not very sensitive to Γ_0 which is included for numerical stability; we use 30 meV, but similar results are found for 5 meV. (To obtain significant damping of the low frequency pole would require making Δ complex.) For Δ , we assume a d-wave gap $\Delta_{\mathbf{k}} = \Delta_{max}(\cos(k_x a) - \cos(k_y a))/2$ with $\Delta_{max} = 32$ meV. The best agreement with experiment is found by choosing the bosonic mode frequency $\omega_0 = 1.3\Delta_{\mathbf{k}}$.

The resulting real and imaginary parts of Σ at \bar{M} are shown in Fig. 3b emphasizing the singular behaviors at Δ due to the Γ_0 term and at $\omega_0 + \Delta$ due to the Γ_1 term. In Fig. 4, we show a comparison of the resulting spectral function (convolved with the experimental energy and momentum resolution) to experimental data at \bar{M} for both wide and narrow energy scans. To aid in the comparison to experiment, a step edge background (which gives a good model of data for $k > k_F$) is added to the calculation. The positions of the sharp peak and the hump obtained from the calculations are compared to the experimental data in Fig. 2. The relative lack of movement of the low frequency peak is well reproduced, as well as its lack of visibility for curves 1 through 3 in Fig. 1b. This lack of movement is due to several factors: (1) the flatness of the band dispersion $\epsilon_{\mathbf{k}}$ near \bar{M} , (2) the lowering of $\omega_0 \sim \Delta_{\mathbf{k}}$ as one moves towards Γ , and (3) the influence of both $Re\Sigma$ and the gap. The last is a new effect worth commenting on. The self-energy (Eq. 2) implies a mass enhancement ($Z > 1$) in the SC state relative to the normal state, which acts to push spectral weight towards E_F . On the other hand, Δ itself pushes spectral weight away from E_F . Thus the dispersion is dramatically flattened relative to the normal state.

We now discuss the p dependence of Σ , which was essentially ignored, except in so far as it was crudely captured by that of ω_0 . Assuming that $Q = (\pi, \pi)$ scattering dominates, as suggested by the neutron data, we would replace $\Gamma_1 N(\omega + \omega_0)$ in Eq. 1 by $g_{p,p+Q}^2 A_{p+Q}(\omega + \omega_0)$ (for $\omega < 0$) where g is the interaction vertex. Assuming a quasiparticle pole approximation for A when solving Eqs. 1 and 2, this would imply a dip in the spectrum at $|\omega| = E_{p+Q} + \omega_0$ where $E_p^2 = \epsilon_p^2 / (ReZ_p)^2 + \Delta_p^2$, and, as before, a persistent low frequency peak if Z is large enough. Note that p and $p + Q$ are coupled in the equation for Σ which requires a numerical solution. Although we leave this complexity for future work, we note that this coupling implies that if a low frequency peak exists for p , then one also exists for $p + Q$ (in fact, they self-consistently generate one another if g is large enough). This is just the effect observed in the data along $(\pi, 0)$ - (π, π) , shown in Fig. 1c, in that a persistent low frequency peak exists for about the same angular range as that along $(\pi, 0)$ - $(0, 0)$. Thus the expected Q dependence of the scattering is indeed reflected in the ARPES data. We note that such scattering can also cause a pairing instability in the d-wave channel.

In conclusion, we have shown the presence of a per-

sistent low frequency peak in photoemission spectra in Bi2212 in the SC state which exists over a large angular range near the \bar{M} point. The dispersion of this feature and the higher binding energy hump as a function of momentum indicates that the electrons in the SC state are interacting with a bosonic mode of resonant character with a frequency between Δ_{max} and $2\Delta_{max}$. Our results once again emphasize that the self-energy is dominated by electron-electron interactions, which is consistent with an electron-electron origin to the pairing.

We thank Yuri Vilk for several stimulating discussions. This work was supported by the U. S. Dept. of Energy, Basic Energy Sciences, under contract W-31-109-ENG-38, the National Science Foundation DMR 9624048, and DMR 91-20000 through the Science and Technology Center for Superconductivity. The Synchrotron Radiation Center is supported by NSF grant DMR-9212658.

-
- [1] M. Randeria *et al.*, Phys. Rev. Lett. **74**, 4951 (1995).
 - [2] Z.-X. Shen and D. S. Dessau, Phys. Rep. **253**, 1 (1995); D. S. Dessau *et al.*, Phys. Rev. Lett. **66**, 2160 (1991) and Phys. Rev. B **45**, 5095 (1992).
 - [3] H. Ding *et al.*, Phys. Rev. Lett. **76**, 1533 (1996).
 - [4] Ch. Renner and O. Fischer, Phys. Rev. B **51**, 2908 (1995).
 - [5] S. Engelsberg and J. R. Schrieffer, Phys. Rev. **131**, 993 (1963); J. R. Schrieffer, *Theory of Superconductivity* (W. A. Benjamin, New York, 1964); D. J. Scalapino, in *Superconductivity*, ed. R. D. Parks (Marcel Dekker, New York, 1969), Vol 1, p. 449.
 - [6] H. A. Mook *et al.*, Phys. Rev. Lett. **70**, 3490 (1993); H. F. Fong *et al.*, Phys. Rev. Lett. **75**, 316 (1995).
 - [7] H. Ding *et al.*, Phys. Rev. Lett. **74**, 2784 (1995).
 - [8] Plots of the width of the low frequency peak versus temperature, based on data from Ref. [1], indicate a dramatic reduction below T_c consistent with microwave conductivity measurements of D. A. Bonn *et al.*, Phys. Rev. Lett. **68**, 2390 (1992).
 - [9] G. B. Arnold, F. M. Mueller, and J. C. Swihart, Phys. Rev. Lett. **67**, 2569 (1991); P. B. Littlewood and C. M. Varma, Phys. Rev. B **46**, 405 (1992); L. Coffey and D. Coffey, Phys. Rev. B **48**, 4184 (1993).
 - [10] S. M. Quinlan, P. J. Hirschfeld, and D. J. Scalapino, Phys. Rev. B **53**, 8575 (1996).
 - [11] E. Demler and S.-C. Zhang, Phys. Rev. Lett. **75**, 4126 (1995); D. Z. Liu, Y. Zha, and K. Levin, Phys. Rev. Lett. **75**, 4130 (1995); N. Bulut and D. J. Scalapino, Phys. Rev. B **53**, 5149 (1996); L. Yin, S. Chakravarty, and P. W. Anderson (unpublished).
 - [12] This form is suggested by the solution of the strong coupling equation for Σ assuming a real, frequency independent gap. We use an s-wave density of states to obtain an analytic result. Results using a d-wave density of states will be qualitatively similar.

[13] C. G. Olson *et al.*, Phys. Rev. B **42**, 381 (1990).

FIG. 1. EDCs in (a) the normal state (105 K) and (b) the superconducting state (13 K) along the line $\Gamma - \bar{M} - Z$, and (c) the superconducting state (13 K) along the line $\bar{M} - Y$, for a slightly overdoped ($T_c = 87\text{K}$) Bi2212 sample with photon polarization $\Gamma - \bar{M}$. The zone is shown as an inset in (c) with the curved line representing the observed Fermi surface.

FIG. 2. Positions (eV) of the sharp peak and the broad hump in the SC state versus normal state peak position. Solid points connected by a dashed line are the experimental data, the solid lines are obtained from the calculations described in the text, and the dotted line represents the normal state dispersion.

FIG. 3. (a) Feynman diagram for the lowest order contribution to the self-energy from electron-electron scattering. The solids lines are electrons, the dashed lines the interaction. (b) $Im\Sigma$ and ReZ at \bar{M} from Eqs. 1 and 2 for the parameter set given in the text.

FIG. 4. Comparison of the data at \bar{M} for (a) wide and (b) narrow energy scans with calculations based on Eqs. 1-3, with an added step edge background contribution.

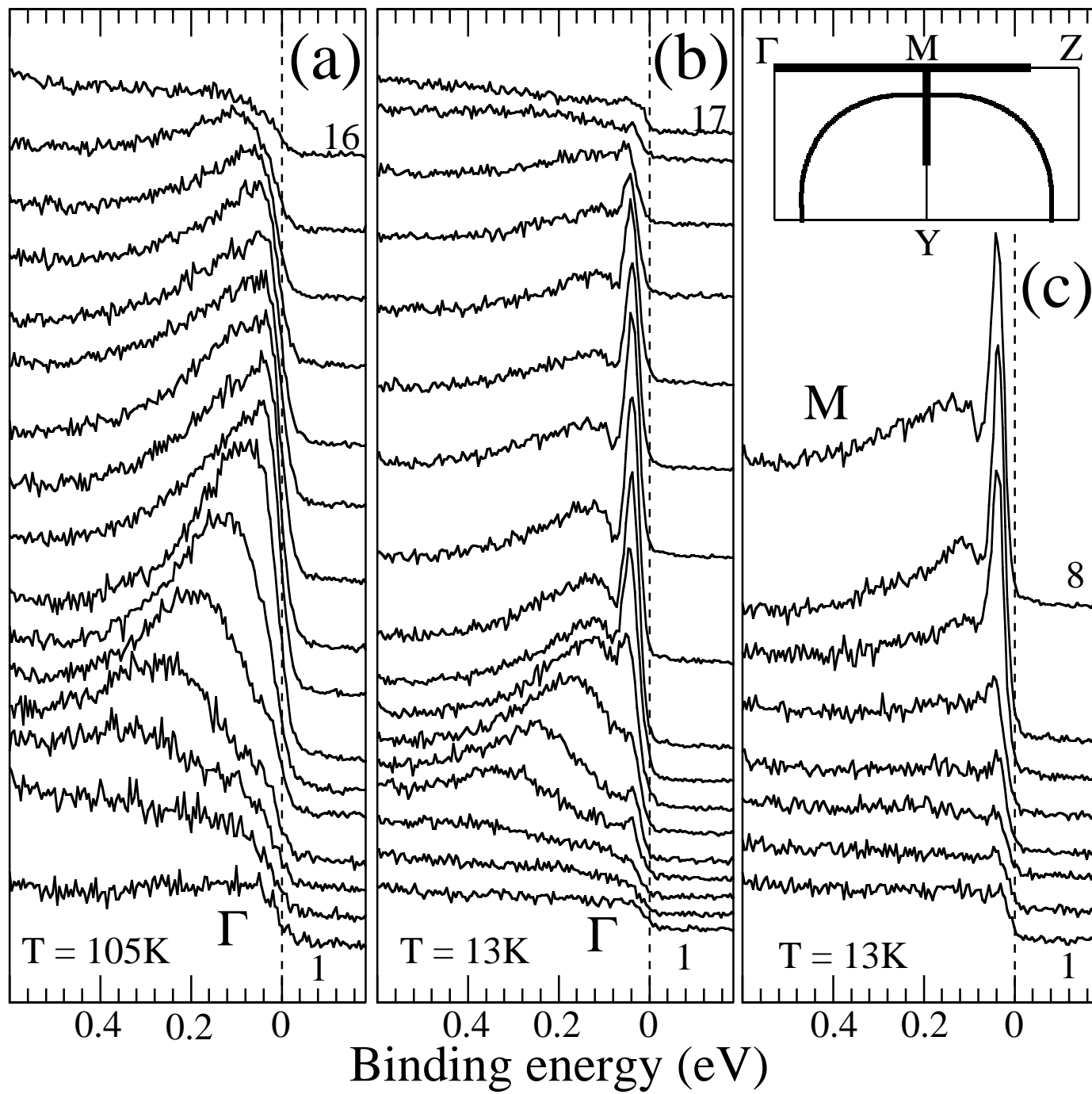


Figure 1 Norman et al

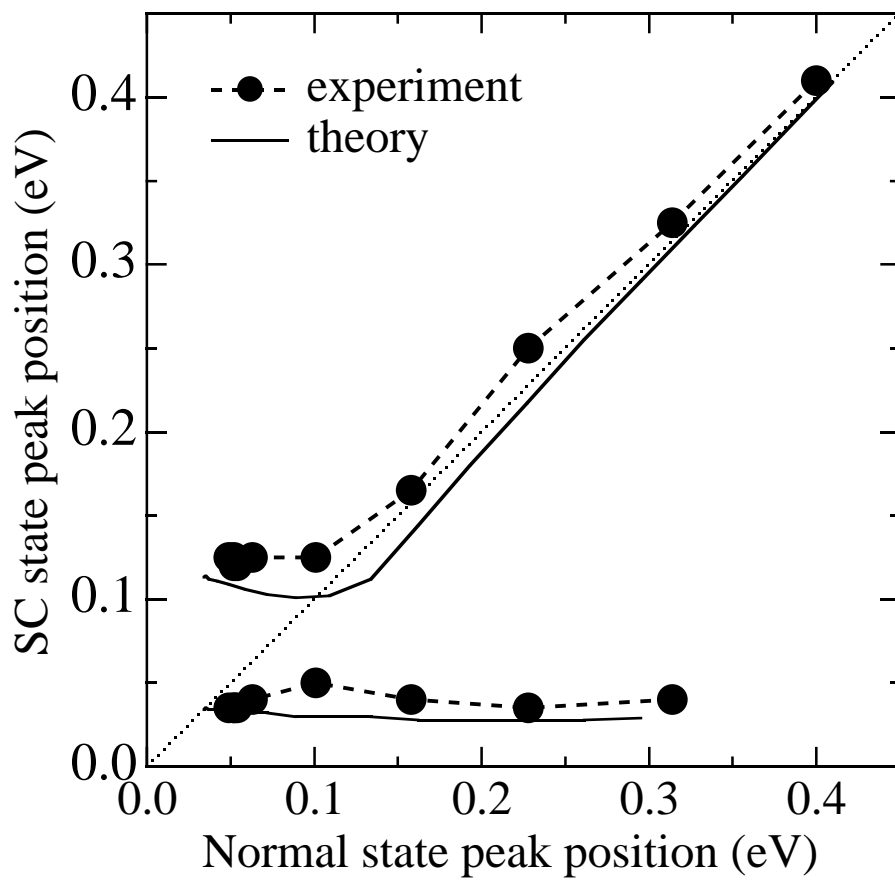


Figure 2 Norman et al.

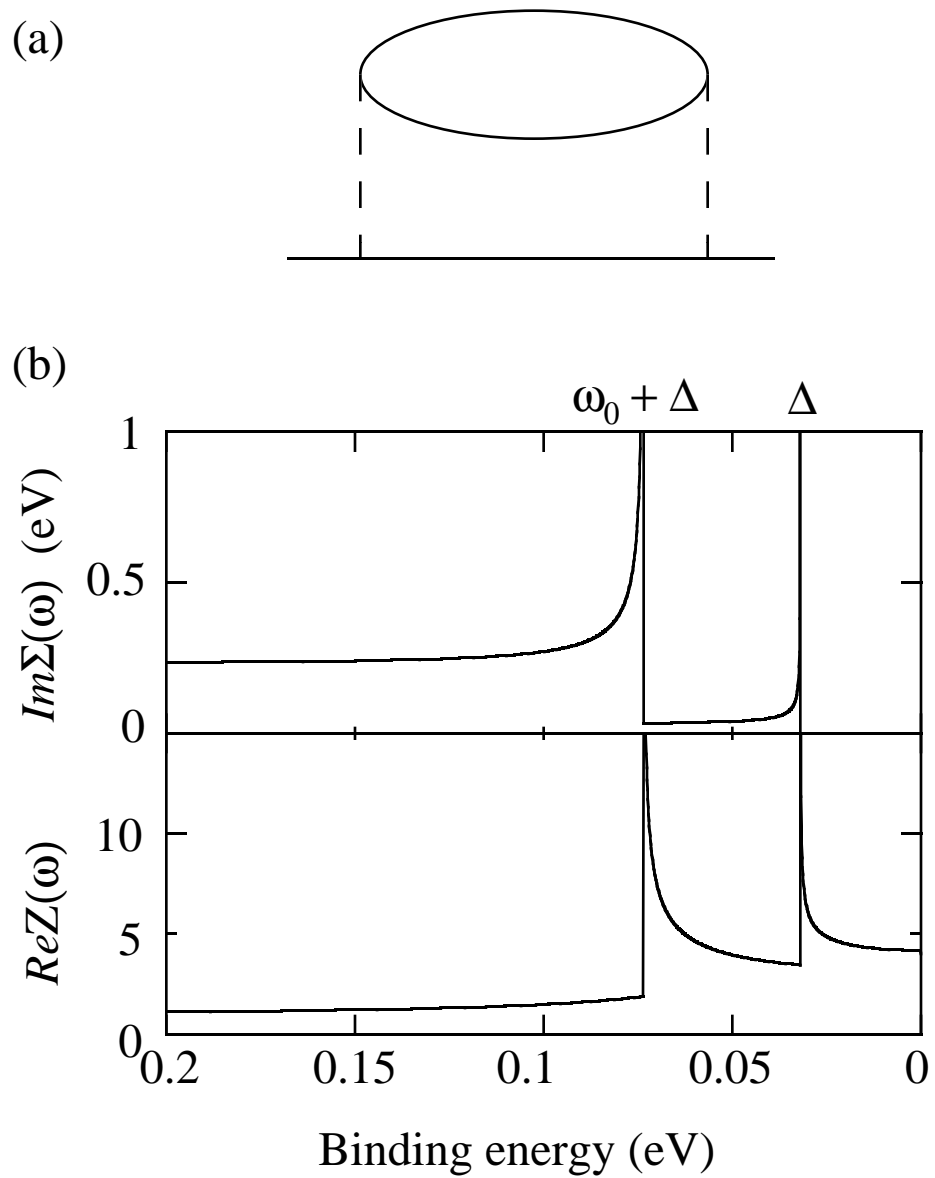


Figure 3 Norman et al.

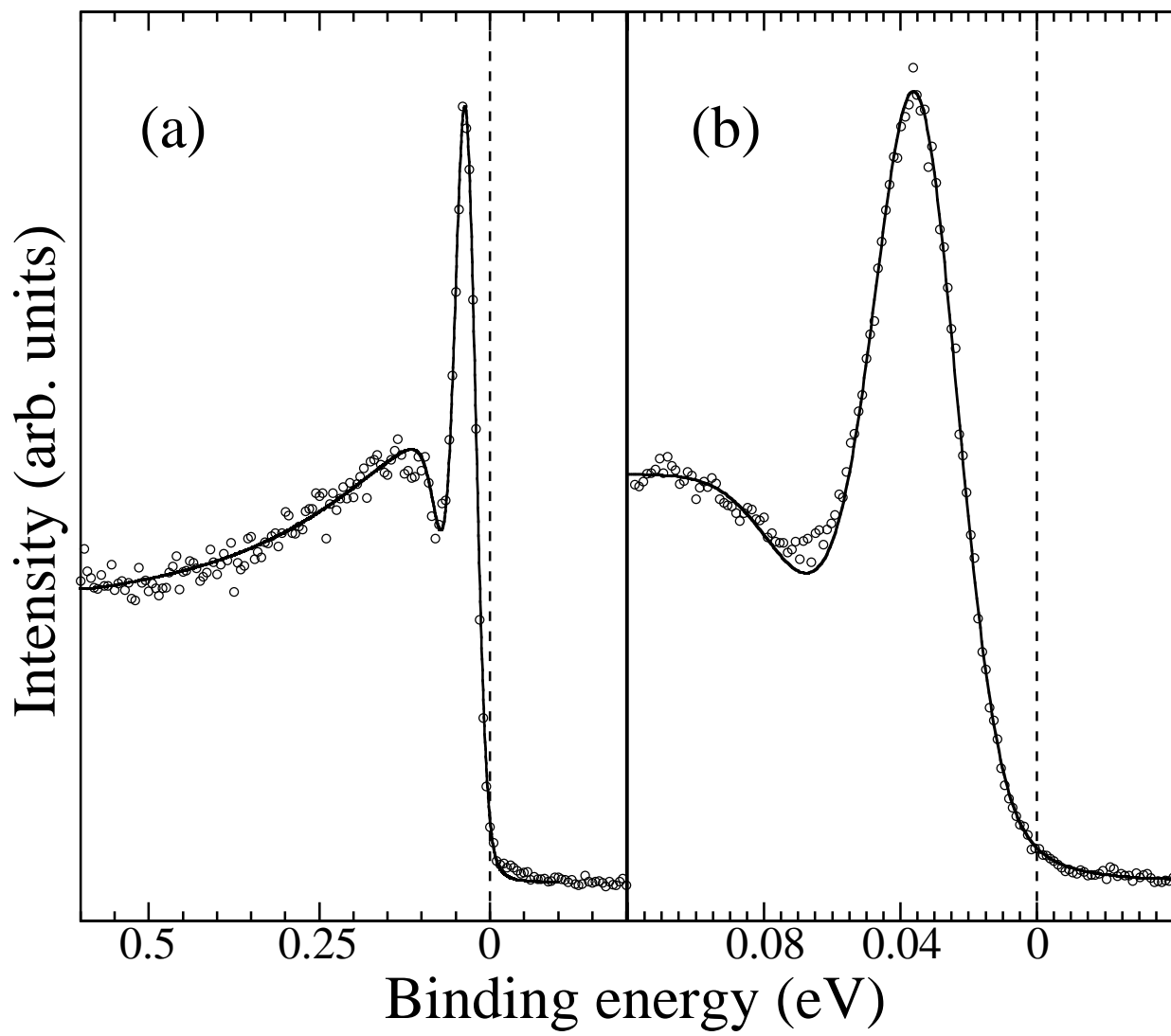


Figure 4 Norman et al.